Received: 7 April 2024 | Revised: 24 May 2024 | Accepted: 25 May 2024

DOI: 10.1002/pen.26817

RESEARCH ARTICLE

POLYMER ENGINEERING AND SCIENCE WILEY

Mechanical and thermal properties of fumed silica-incorporated silane-terminated urethane/epoxy-interpenetrating polymer network nanocomposites

Emre Akın | **Mustafa Çakır** | **İlyas Kartal**

Faculty of Technology, Metallurgical and Materials Engineering, Marmara University, Istanbul, Turkey

Correspondence
Emre Akın, Faculty of Technology, Metallurgical and Materials Engineering, Marmara University, Istanbul, Turkey
Email: emre.akin@marmara.edu.tr

Abstract

In this study, it was aimed to improve the mechanical and thermal properties of epoxy materials based on diglycidyl ether of bisphenol-A-based. For this purpose, three different nanocomposite materials were prepared at various ratios including a fumed silica nanoparticle-reinforced epoxy nanocomposite (FSN), an epoxy/silane-terminated urethane (STU) hybrid interpenetrating polymer network (IPN) nanocomposite (SHIN), and a fumed silica-reinforced epoxy/STU hybrid IPN nanocomposite (FSHIN). While synthesizing SHIN, 3-isocyanato propyl trimethoxy silane (ICPTMS) and poly (hexamethylene carbonate) diol were used. The synthesized STU polymer chains were crosslinked by reacting them with TEOS via the sol–gel process. Therefore, hybrid networks were obtained. Moreover, fumed silica nanoparticles were incorporated into the hybrid networks via the sol–gel process for FSHINs. The three different nanocomposite materials exhibited much more improved properties than the neat epoxy. The most prominent nanocomposite was FSHIN. In comparison with the neat epoxy, Young's modulus, ultimate tensile strength, and Izod impact resistance values increased at ratios of 53%, 50%, and 223%, respectively. Glass transition temperature values and char yield values increased substantially in all nanocomposites. However, thermal decomposition temperatures increased only for FSNs. Moreover, these values for FSHINs that were very close to those of the neat epoxy were considerably higher than those of SHINs.

Highlights

- Fumed silica-incorporated silane-terminated urethane/epoxy IPN nanocomposites.
- Substantially improved mechanical properties and impact resistance.
- Improved thermal stability.

KEYWORDS

hybrid networks, interpenetrating polymer networks, nanocomposite, silane-terminated urethanes

1 | INTRODUCTION

Epoxies are a superior form of thermosetting polymers in terms of properties such as high tensile strength, stiffness, hardness, and low shrinkage during the curing process. Moreover, an epoxy material exhibits good thermal and dimensional stability, as well as high resistance to moisture, corrosion, and chemicals. These unique properties have been attractive considerably for their widespread engineering applicability. Various epoxy structures and composites are widely used in different industrial areas because of their structural characteristics. However, there are some constraints about neat epoxy polymers such as low fracture resistance and undesirable brittleness properties due to the high crosslink density of the epoxy network.[1,2] These constraints have limited their engineering applications. For this reason, studies have focused on improving these constraints of epoxies with nanocomposite and composite applications besides the improvement of their mechanical properties.[3–5]

Until this time, some studies have been conducted with various structures by incorporating long hydrocarbon chains, different reinforcing organic or inorganic nanoparticles, rubber, and thermoplastics into the epoxy matrix to improve the mechanical properties of the matrix. In particular, current advanced nanotechnology has allowed the improvement of the properties of epoxies with nanoparticles such as carbon nanotubes and silica nanoparticles to achieve superior properties.[1,2] There are lots of reports in the literature about nanoparticles such as SiO_2, ZnO, TiO_2, graphene oxide, carbon nanotube, boron nitride, and nanoclay stating that these materials could improve the mechanical properties of elastomers, polyurethane, and epoxy by increasing their compatibility with the polymer matrix.[5–7] However, the properties of nanocomposite materials can be worsened due to the considerably high aggregation tendency of nanoparticles. Therefore, there are several serious efforts to prevent aggregation and improve the properties of nanocomposites by providing homogeneous dispersion and strong compatibility with the matrix.[8,9]

The sol–gel process is widely used to obtain organic–inorganic hybrids as a proper matrix for composites thanks to its unique properties. This process generally includes hydrolysis and condensation reactions to form Si—OH and Si—O—Si bonds. As a result of this process, Si—O—Si bonds can be created between polymer chains. At the same time, nanoparticles can be bonded covalently between organic and inorganic structures by creating strong interfacial strength with the matrix due to the functional groups on their surfaces. Therefore, a more homogeneous dispersion of nanoparticles can be achieved by minimizing the agglomeration of the nanoparticles.[5,9,10]

In addition to the homogeneous dispersion of nanoparticles with silane groups through the sol–gel process, the occurrence of interpenetrating networks (IPNs) with low molecular chains in structures can increase the mechanical properties and fracture toughness instead of the incorporation of long molecular chains with flexible groups. This is because polymers with long molecular chains in the main structure or matrix can cause an undesired increase in viscosity.[2] Therefore, researchers have focused on IPNs. IPNs are described in the literature as a unique kind of polymer alloy. They have chemically dissimilar crosslinked polymer chains, and they are entangled at a molecular scale in the network of the secondary polymer chain.[1,3] Moreover, IPNs generally exhibit excellent properties due to their multiple networks, and composites with IPNs generally exhibit higher strength, toughness, and wear resistance than other particle/matrix-type composite structures.[1,11]

On the contrary, inorganic structures can improve thermal properties thanks to their components providing high dissociation energy such as Si—O—Si bonds. The dissociation energy of Si—O bonds (ca. 460.5 kJ mol^{-1}) is higher than those of C—O (358 kJ mol^{-1}), C—C (304 kJ mol^{-1}), and C—NH (98 kJ mol^{-1}) bonds. Moreover, these Si—O bonds can affect the properties of the materials as they exhibit low free surface energy, flexibility, and abrasion characteristics.[5,8,12]

The purpose of this study is to obtain novel epoxy nanocomposites with enhanced mechanical and thermal properties. In this regard, three different nanocomposite materials were produced. These were a fumed silica nanoparticle-reinforced epoxy nanocomposite (FSN), an epoxy/silane-terminated urethane (STU) hybrid interpenetrating polymer network (IPN) nanocomposite (SHIN), and a fumed silica-reinforced epoxy/STU hybrid IPN nanocomposite (FSHIN). In the synthesis of SHIN, 3-isocyanato propyl trimethoxy silane (ICPTMS) and poly (hexamethylene carbonate) diol were used. The synthesized STU polymer chains were crosslinked by reacting them with TEOS via the sol–gel process. Therefore, hybrid networks were obtained. On the contrary, fumed silica nanoparticles were pretreated with ethanol and incorporated into the hybrid networks via the sol–gel process to obtain FSHINs. These three different nanocomposites were compared with each other and the neat epoxy. The samples were mechanically characterized via tensile and Izod impact resistance tests. Thermal decomposition temperatures and char yields were observed by thermogravimetric analysis (TGA), and glass transition temperature (T_g) values were observed by differential scanning calorimetry (DSC). These samples were prepared at various ratios including 2, 4, 6, 8, and 10 wt%. Particle dispersion properties and fracture surface

morphologies were characterized by scanning electron microscopy (SEM). Among these nanocomposites, FSHINs came to the fore in terms of Young's modulus, ultimate tensile strength, and Izod impact resistance properties. They presented increases at ratios of 53%, 50%, and 223%, respectively. In addition to these, T_g values and char yields improved significantly. Thermal decomposition temperatures decreased slightly, but the values of FSHINs were considerably high. These values were very close to those of the neat epoxy.

2 | MATERIALS AND METHODS

2.1 | Materials

The epoxy resin EPIKOTE 828 based on a diglycidyl ether of bisphenol-A-based reactive resin and its curing agent EPIKURE F205 hardener were purchased from Hexion. BDMA (Benzyl dimethylamine) accelerator, tetrahydrofuran (THF), dimethylformamide (DMF), poly (hexamethylene carbonate) diol (Mn: 2000), 3-isocyanatopropyltrimethoxysilane (ICPTMS), tetraethoxysilane (TEOS), ethanol, and p-toluenesulfonic acid (PTSA) and dibutyltin dilaurate (DBTL) as catalysts were purchased from Aldrich. Teflon molds were purchased from APT PTFE parts. Pyrogenic silica–fumed silica HDK N20 nanoparticles were purchased from Wacker Chemie, Munich, Germany. HDK N20 is a hydrophilic silica material whose primary particle size is reported to be 5–30 nm. The hydrophilic silica (N20) is produced by the hydrolysis of chlorosilanes in an oxyhydrogen flame. It consists of >99.8% amorphous silicon dioxide by weight and has a silanol content of 2SiOH/nm.[2,13] Table 1 shows the properties of the HDK N20 fumed silica nanoparticles. All materials were used as received.

2.2 | Modification of fumed silica

To increase the wettability and dispersivity of the fumed silica in the epoxy matrix, unmodified fumed silica particles were mixed with ethanol using a mechanical stirrer for 4 h in a beaker to prepare a % wt/wt fumed silica/ethanol suspension at an equal ratio. This solution was then exposed to an ultrasonic bath to minimize the agglomeration of the particles. Finally, the suspension was heated at 40°C in a drying vacuum oven for 30 min. The fumed silica particles were prepared to be added into the epoxy resin.

TABLE 1 Properties of HDK N20 (hydrophilic) fumed silica.

Property	Inspection method	Value
BET surface	DIN ISO 9277 DIN 66132	175–225 m^2/g
Loss on drying	DIN EN ISO 787-2	<1.5%
Sieve residue	DIN EN ISO 787-11	<0.03%
Tamped density	DIN EN ISO 787-9	40 g/L
pH		3.8–4.3

2.3 | Preparation of fumed silica nanoparticles reinforced with epoxy nanocomposite

Fumed silica, which is referred to as pyrogenic silica due to its flame-produced nature, is composed of small amorphous silica droplets that fuse to form three-dimensional secondary particles that are branching and chain-like, before aggregating into tertiary particles. The fumed silica nanoparticles were added to the epoxy resin and stirred mechanically as homogeneously as possible for 5 h. After this process, degassing process was carried out at 40°C to remove bubbles from the filled epoxy resin in the drying vacuum oven. Then, the curing agent was added stoichiometrically. Epoxy system was stirred homogeneously for 20 min. Before pouring the homogeneous mixture into Teflon molds, BDMA was added as an accelerator and stirred for 5 min. The poured mixtures were cured at room temperature for 5 h. The samples taken from the molds were degassed at 80°C in the drying vacuum oven for a day to remove the residual ethanol, solvent, and moisture. The fumed silica nanoparticles were introduced into the epoxy systems at ratios varying from 2 to 10 wt%.

2.4 | Synthesis of silane-terminated urethane polymer

Poly (hexamethylene carbonate) diol (0.025 moles) and 3-isocyanatopropyltrimethoxysilane (ICPTMS) (0.05 mole) were charged to a 250 mL three-neck round-bottom flask, equipped with a thermometer pocket, a water condenser, and a magnetic stirrer, and finally, filled with 100 mL DMF/THF (1 wt./1 wt.). Dibutyltin dilaurate, at a concentration of 0.3 wt%, was added to the reaction flask as a catalyst. The temperature was raised to 60°C, and the mixture was stirred for 24 h. As a result of these reactions, the STU polymer, which had a silane-terminated urethane functional group at both ends of the chain, was synthesized. The completion of the reaction was confirmed by the disappearance of the characteristic —NCO peak at 2275 cm^{-1} in the FTIR spectrum as shown in Figure 1. The resultant mixture was stored in a refrigerator at +4°C.

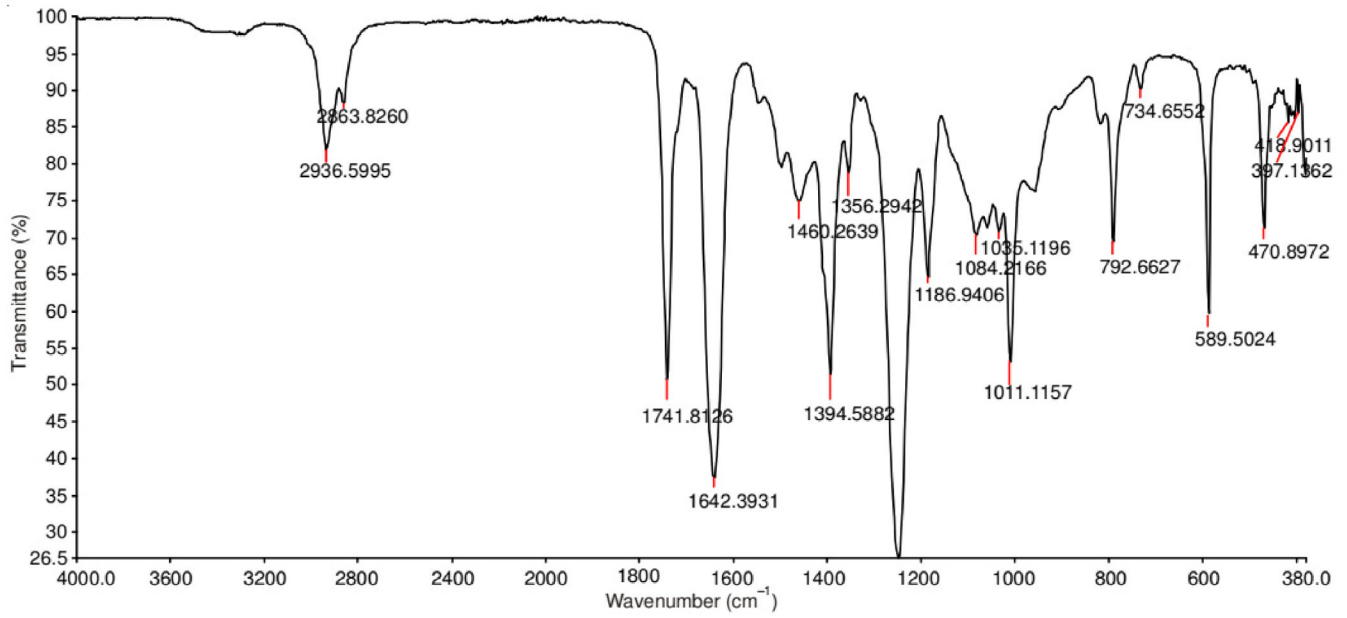

FIGURE 1 FTIR spectrum of silane-terminated urethane polymer.

2.5 | Hydrolysis of TEOS

TEOS, water, and p-toluene sulfonic acid in ethanol were mixed at room temperature. The pH of the system was measured as 3.5–4. The water/silicate ratio was calculated as $r = 3$. The mixture was left overnight at room temperature.

2.6 | Preparation of epoxy/STU hybrid IPN nanocomposite

The prepared solutions of STU polymer and the pre-hydrolyzed TEOS solution were mixed for 2 h. The mixture was prepared by reacting 4 mole equiv. of the pre-hydrolyzed TEOS solution with 1 mole equiv. of the STU polymer. This solution was added into the prepared epoxy systems before gelation in different ratios that varied 2–10 wt% consecutively and stirred until they were homogeneous. BDMA was added as an accelerator and stirred for 5 min. After stirring of the added solutions and epoxy systems, it was heated at 40°C in a drying vacuum oven for 15 min for the degassing of the solution. Finally, the solutions were poured into Teflon molds and cured at room temperature for 5 h. The added weight contents were calculated according to the solid content of the hydrolyzed STU polymer and TEOS solution. The solid weight ratio of this solution was adjusted as 50 wt%. The stirring of the STU polymer and pre-hydrolyzed TEOS solutions was performed to hydrolyze silane groups of the STU polymer. Following this hydrolysis process, the second phase that is gelation of the sol–gel process was carried out simultaneously with the epoxy system's curing. It is expected that hydrolyzed TEOS and STU polymer formed partly silica particles in IPN structures before or during gelation by sol–gel technique. Consequently, sol–gel technique was used to produce both partly silica particles and IPN structures in a single system. The representative STU hybrid network structure of the final products is given in Figure 2.

2.7 | Preparation of fumed silica-reinforced epoxy/STU hybrid IPN nanocomposite

The prepared solutions of the STU polymer, hydrolyzed TEOS, and fumed silica nanoparticles were mixed together for 2 h. The mixture of the solutions was prepared by reacting 4 mole equiv. of hydrolyzed TEOS with 1 mole equiv. of the STU polymer. Besides, 1 wt. equiv. of STU polymer was added with 1 wt. equiv. of the fumed silica nanoparticles into the hybrid polymer solutions. The ratios of this solution were then changed from 2 to 10 wt% consecutively, they were added into the epoxy systems, and stirred until they were homogeneous. It was thought that the homogeneous dispersion of the fumed silica nanoparticles would be provided with the hydrolyzed TEOS. After stirring, the degassing process was applied at 40°C in a drying vacuum oven for 15 min. Finally, the mixture was poured into Teflon molds. The flow diagram of the preparation of the FSHIN samples is given in Figure 4. Moreover, the representative structure of the fumed silica-reinforced STU hybrid network is given in Figure 3.

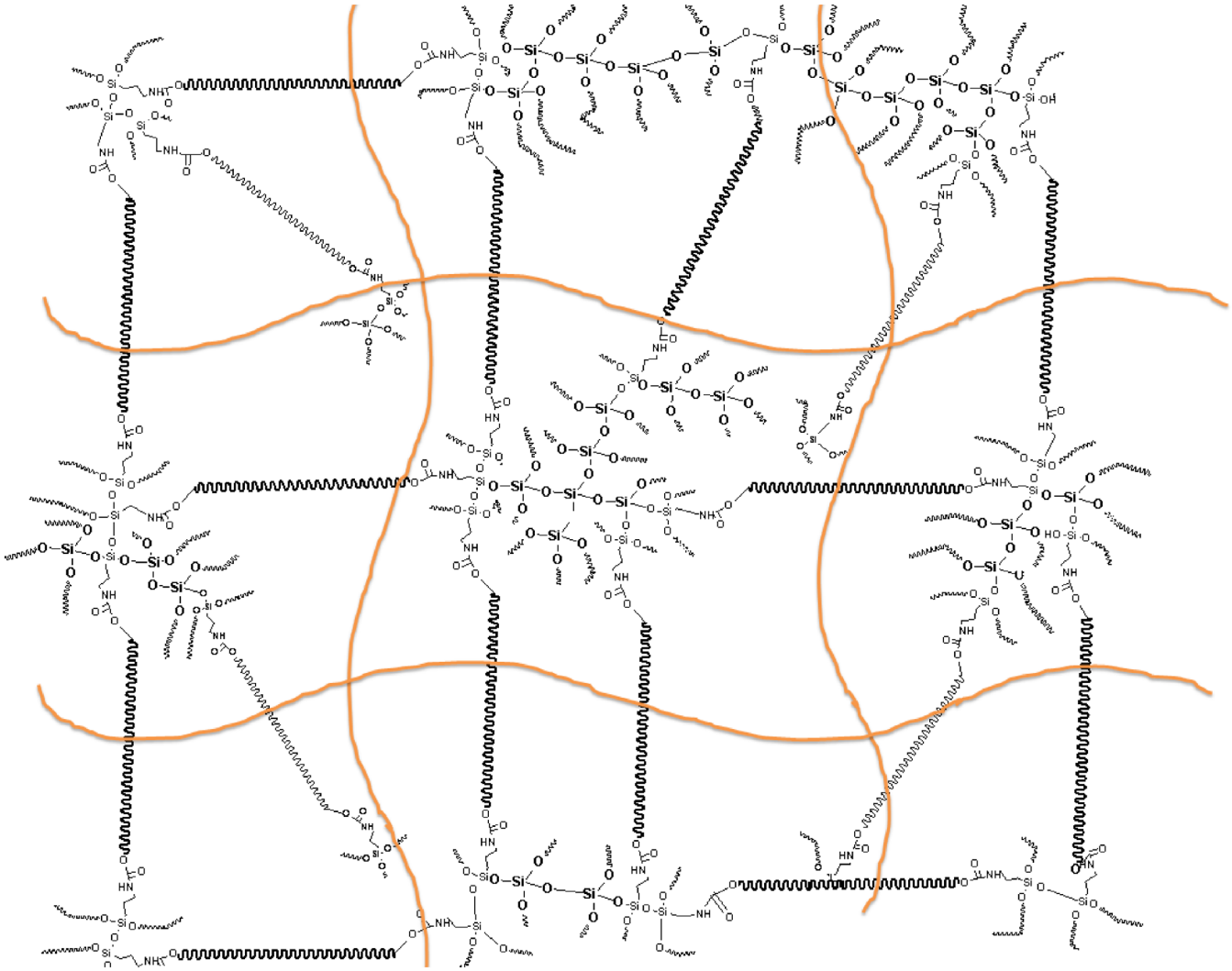

FIGURE 2 Representative structure of silane-terminated urethane hybrid network in epoxy network.

2.8 | Characterization of test specimens

Three samples were prepared for each wt% value. The average of these three values was used for the results. Analyses were conducted based on the average results. The coefficients of variation (CoV) are presented in Table 2, Figure 5, and Figure 6. CoV is the ratio of the standard deviation to the mean of the results of a sample multiplied by 100 that is given in Equation (1). In this equation, s is the standard deviation, and μ is the mean of the values of a sample.

$$\text{coV} = \frac{s}{\mu} \times 100. \quad (1)$$

CoV is a measure of relative event dispersion and is generally used for comparing relative risk. It can also be used to evaluate quantitative likelihood or probability distributions. CoV measures the spread of values like standard deviation. While standard deviation measures distance from the mean, CoV measures the ratio of the standard deviation to the mean.

The samples were characterized mechanically and thermally. The fractured surfaces were observed by SEM. To characterize the mechanical properties of the FSN, SHIN, and FSHIN samples, standard tensile tests were applied. In these tests, Young's modulus, ultimate tensile strength, and elongation at break values were measured according to ASTM D638. The tensile tests were performed using Zwick Z010 equipment at room temperature at a crosshead speed of 5 mm/min.

Izod impact strength was measured using unnotched samples according to ASTM D 4812-99 with a CEAST Resil impact analyzer (Junior) and a 5.4J hammer at a striking rate of 3.96 m/s. The fracture surface morphology tests of the specimens were performed using a field emission scanning electron microscope (FESEM) (Carl Zeiss Ultra Plus) device at an acceleration voltage of

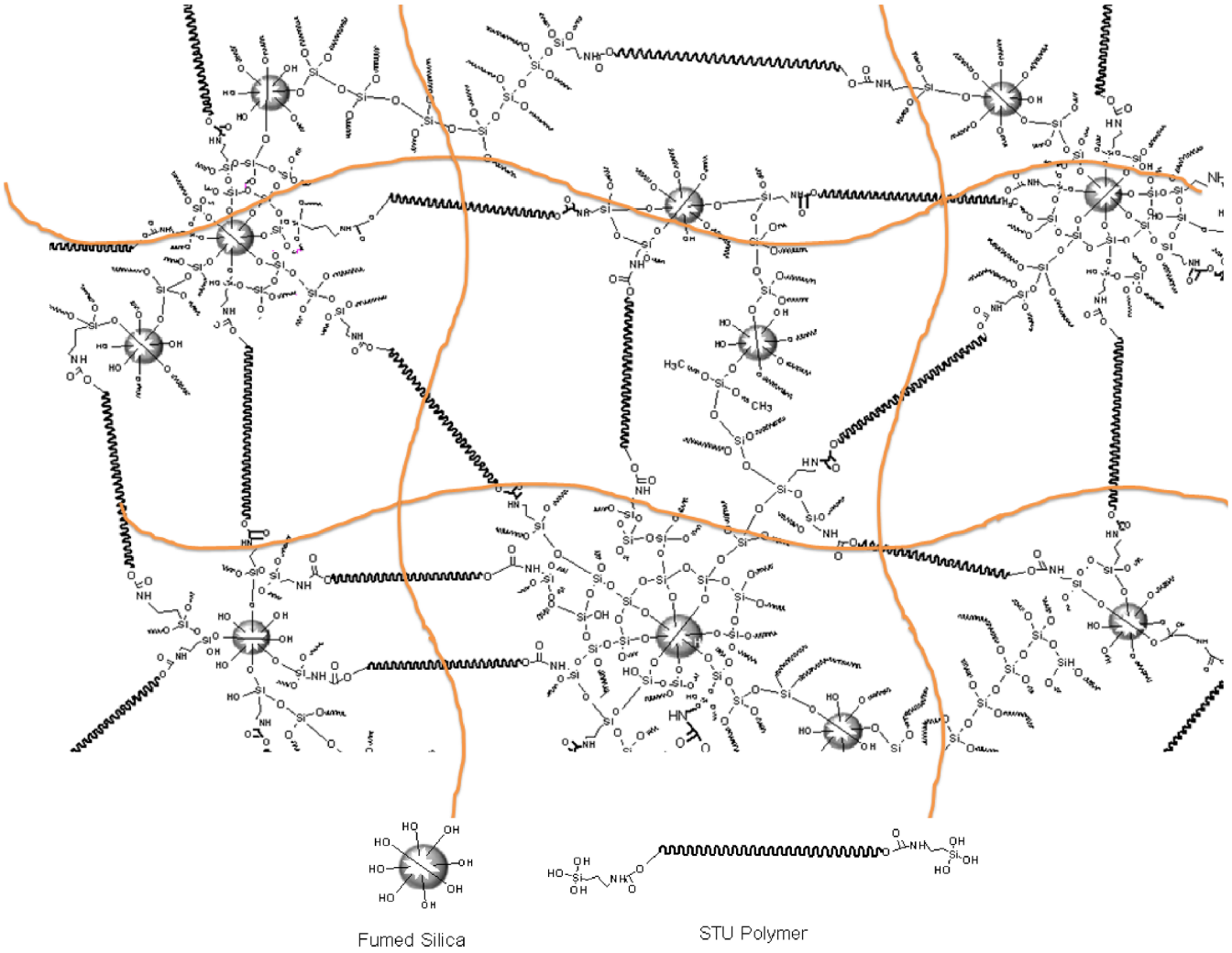

FIGURE 3 Representative structure of fumed silica-reinforced silane-terminated urethane hybrid network in epoxy network.

20 kV with an energy-dispersive X-ray spectroscopy (semi-quantitative EDX) analysis system. The specimens were coated with 2–4 nm of Au/Pd in an ion beam sputtering system via a Quorum Q150R machine before SEM examinations. The FTIR spectra of the STU polymer were recorded using a Shimadzu 8300 FT-IR spectrophotometer. The TGA of all samples were performed using a TA Instruments Q50 model device. The samples were run from 30 to 800°C at a heating rate of 10°C/min under a nitrogen atmosphere.

3 | RESULTS AND DISCUSSION

In our study, three different reinforcement methods were applied to epoxy systems, including fumed silica nanoparticles, an STU organic–inorganic hybrid IPN structure, and a fumed silica-reinforced STU organic–inorganic hybrid IPN structure. All reinforcement systems were introduced into the epoxy systems at ratios varying from 2 to 10 wt%.

3.1 | Mechanical properties

Mechanical properties were investigated with tensile and Izod impact tests for all reinforcement systems. The obtained tensile and impact test values are shown in Table 2. In the examinations of the FSN samples, the increase in fumed silica content only increased the Young's modulus significantly. The Young's modulus showed a maximum increase of 58% with the increase in FSN content. Other mechanical properties increased slightly up to the ratio of 6 wt%, including ultimate tensile strength and Izod impact resistance. Ultimate tensile strength values showed an increase of 9.75%. On the contrary, elongation at break values continuously decreased with the content of FSN, and the maximum decrease was observed as 19%.

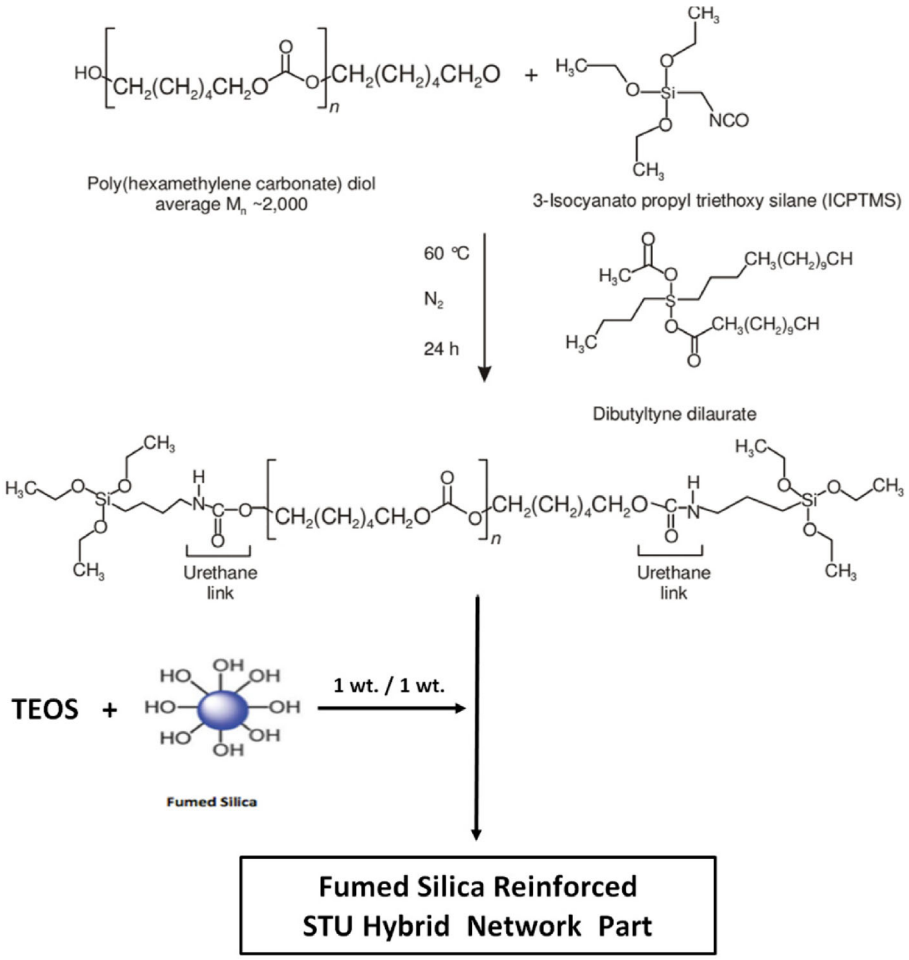

FIGURE 4 Preparation of fumed silica-reinforced hybrid network structure.

Marouf et al.[14] reported that micro-sized particle-reinforced polymers were effective on crack growth behavior, and they increased fracture toughness. The fracture toughness of the polymer nanocomposite was increased along with the sizes of the reinforcing silica particles between 2 and 47 μm. In the range of 200–1560 nm, the silica particles had a negative effect on the polymer nanocomposite. Moreover, the reinforcement particle sizes in the range of 20–170 nm showed little or no effect in terms of fracture toughness. Liang and Pearson incorporated silica particles with particle sizes of 20 and 80 nm into an epoxy system, and they found similar results.[14] On the contrary, Marouf et al.[14] also stated that the uniform dispersion of the fillers was a very important parameter to obtain high fracture toughness values when the volumetric fraction of the particles was high. Otherwise, fracture toughness values would decrease due to the agglomeration at high filler loading values.

In this study, the impact resistance values of FSNs showed little increase (3.3%), and the resistance decreased at larger content values than 6%. FSNs showed particle sizes varying from 5–30 to 70 nm when the content increased. As shown in the SEM micrograph of FSN10 in Figure 7, nanoparticle sizes became approximately 70 nm. Little agglomeration was seen at larger content values than 6%. On the contrary, until the content value of 6%, the dispersion of the fumed silica was homogeneous, as seen in Figure 7. Therefore, the impact resistance could be decreased for FSN8 and FSN10 due to agglomeration and the less homogeneous dispersion in the samples.

During the production of the second set of nanocomposite materials, namely SHINs, poly (hexamethylene carbonate) was used as a soft segment crosslinked by Si—O—Si bonds. For this purpose, poly (hexamethylene carbonate) was terminated by silane groups using ICPTMS. Therefore, silane-terminated urethane-containing poly (hexamethylene carbonate) was obtained. The component was then hydrolyzed with the pre-hydrolyzed TEOS (pH: 4–4.5) in a beaker by the sol–gel process. After stirring the mixture for 4 h without condensation and gelation, the hybrid system was incorporated into the epoxy system to obtain simultaneous interpenetrating polymer networks at various ratios.

The mechanical properties of the samples in the system, namely SHINs, such as ultimate tensile strength, elongation at break, Young's modulus, and Izod impact resistance, were observed. Ultimate tensile strength and

TABLE 2 Mechanical properties of nanocomposites.

Samples	Young's modulus (MPa)	CoV	Elongation at break (%)	CoV	Ultimate tensile strength (MPa)	CoV	Izod impact (kJ/m^2)	CoV
EPOXY	1881	3.4	3.1	3.3	41	6.7	9.1	6.5
FSN2	2117	11.5	3.0	2.5	42.2	5.5	9.3	7.5
SHIN2	1780	4.4	4.3	4.1	39.2	4.1	11.7	6.1
FSHIN2	1983	6.8	3.8	3.3	46.7	4.2	15.3	18.1
FSN4	2523	16.1	2.7	6.4	43.5	2.2	9.4	15.3
SHIN4	1661	3.1	5.2	3.8	35.1	5.9	12.8	18.9
FSHIN4	2347	9.0	4.3	3.4	54.8	4.6	16.1	9.9
FSN6	2736	10.4	2.5	6	43.9	7.4	9.4	23.6
SHIN6	1524	7.51	6.5	2.7	33.1	7.9	14.5	15.1
FSHIN6	2586	6.3	5.3	2.4	56.3	4.3	24.2	19
FSN8	3080	7.2	2.4	4.3	42.3	7.1	8.3	9.2
SHIN8	1387	10.6	7.6	1.7	31.4	12.5	15.5	14.8
FSHIN8	2754	8.7	6.3	1.4	61.6	6.3	29.3	20.5
FSN10	3095	4.9	2.4	2.7	40.4	4.7	7.4	13.3
SHIN10	1218	17.3	8.5	3	28.3	15	16.8	8.6
FSHIN10	2889	9.8	6.2	2.2	60.4	5.3	27.2	11.2

Young's modulus decreased continuously as shown in Figures 5 and 6. The Young's modulus and ultimate tensile strength values showed decreases by 35% and 32%, respectively, with the increasing SHIN content. On the contrary, the Izod impact resistance values increased continuously, and this increase was 46% for SHIN10. Considering these results, the decrease in the ultimate tensile strength and Young's modulus values could be associated with the soft segments poly (hexamethylene carbonate) and Si—O—Si bonds. This second phase could have prevented the rigidity of the epoxy system.

This second phase included in the Si—O—Si bonds containing the poly (hexamethylene carbonate) structure is shown in Figure 2. Si—O—Si bonds could have made both linear and crosslink covalent bonds with the poly (hexamethylene carbonate) chain. Moreover, Si—OH groups might have reacted with hydroxyl groups on the epoxy backbone at the same time.[15] Hence, the soft segment containing an interpenetrating polymer network system was obtained. This structure was softer and had less rigidity than the epoxy system according to the results. The siloxane moiety and soft segment of poly (hexamethylene carbonate) of the system exhibited an energy-dissipating characteristic, increasing the impact resistance and elongation at break values. The dominant effect of the soft segments was observed in the structure. It was thought that Si—O—Si linear bonds could have occurred rather than silica particles and networks because of the decreases in the Young's modulus and tensile strength.

The third nanocomposite material, FSHIN, was produced to eliminate the drawbacks of the other materials (FSNs and SHINs) and obtain improved mechanical properties. While producing this material, it was aimed to incorporate fumed silica particulates covalently into the STU hybrid structure. For this purpose, TEOS was first hydrolyzed at 3.5–4 pH. After the hydrolysis of TEOS in ethanol by adjusting the pH of TEOS to 4.5, the STU hybrid polymer and the fumed silica particles were added to the pre-hydrolyzed TEOS solution and stirred for 2 h. This solution was then mixed with an epoxy system to obtain the fumed silica-reinforced simultaneously interpenetrating polymer network. It was thought that fumed silica particles could be formed with covalent and physical bonds in the hybrid IPN structure as shown in Figure 3. Inorganic silica particles could be larger than those in the FSN samples due to the bonding of the fumed silica particles with TEOS groups. Because of this, the particle size distribution was not expected to be homogeneous. The second phase can also be observed in the SEM micrograph in Figure 9.

As in the cases of FSNs and SHINs, the mechanical properties of FSHINs were also observed. Ultimate tensile strength increased up to the sample with a content of 6%, and then, a decreasing trend was observed as shown in Figure 5. The increase at 6 wt% was found to be 50% compared with FSN0. At the same time, the Young's modulus values showed a large increase up to the sample with a content of 8%, and then, a more stable increase was seen up to the sample with a content of 10% as shown in

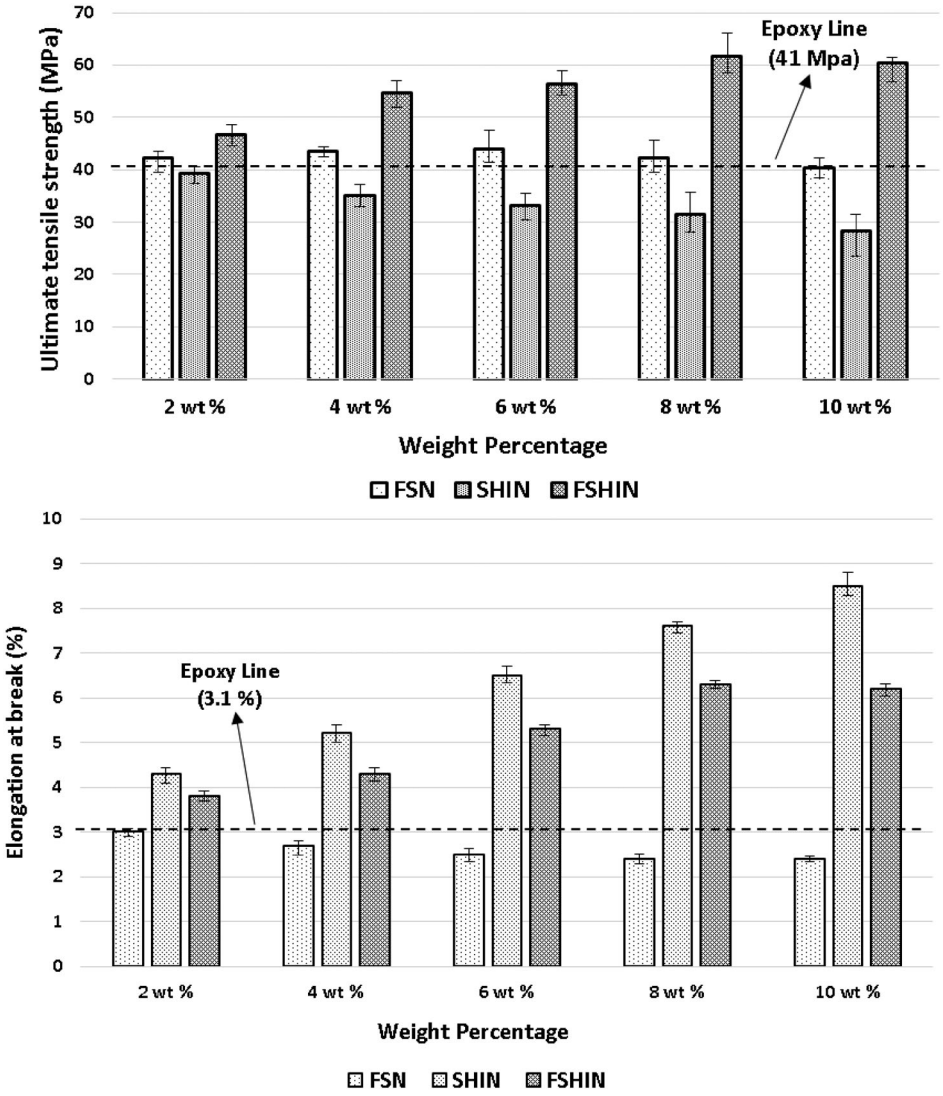

FIGURE 5 Elongation at break and ultimate tensile strength values of nanocomposites.

Figure 6. FSHIN10 showed an increase in Young's modulus by 53%.

It was thought that fumed silica particles formed in the second hybrid IPN phase and matrix. The fumed silica particles incorporated into the second phase could have increased the rigidity of the second phase. It may also be thought that the extent of Si—O—Si bonding between the STU polymers may have decreased due to the possibility of a reaction of the hydrolyzed TEOS with Si—OH groups on the fumed silica particles. This situation could also have reduced the soft segment effect of Si—O—Si bonds in addition to reinforcing the effect of the fumed silica particles in the hybrid system.

The largest increase in the ultimate tensile strength values was observed for FSHINs, and this situation could have been derived from the improved compatibility of the fumed silica particles with the system.

In the comparisons of the FSNs and FSHINs with each other, the weight ratios of the fumed silica particles in FSNs added into the epoxy system were larger than those in FSHINs for each sample content percentage. The weight ratio was calculated as 4.65/1 (FSN/FSHIN). All stoichiometric weight and molar ratios are given in Table 3. The Young's modulus values of all FSHINs were found between the values of SHINs and FSNs due to the incorporation of the fumed silica particles. There are two factors that could have affected this result: the decrease in the weight ratio of the fumed silica particles belonging to FSHINs compared with FSNs and the soft segments of the STU polymer. Another important result was the elongation at break value for FSHINs. FSHINs exhibited high elongation values in addition to their ultimate tensile strength and Young's modulus. This value increased up to FSHIN8 and showed a little decrease at larger content values. This increase was 103%. These values were close to the elongation at break values of SHINs. It can be deduced that the soft segments of the STU hybrid polymer structure in FSHINs were still dominant. In light of

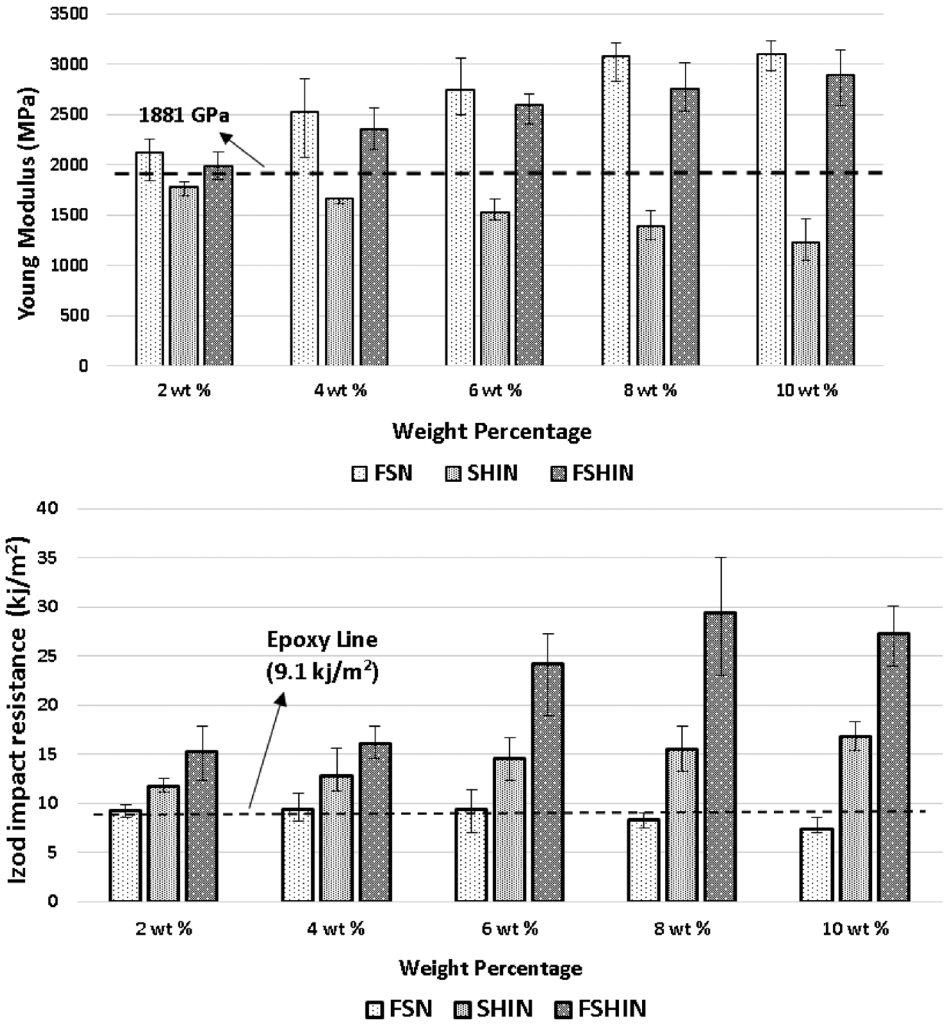

FIGURE 6 Young's modulus and Izod impact resistance values of nanocomposites.

these results, Izod impact resistance improved significantly with the fumed silica-reinforced STU polymer hybrid structure. The resistance showed a substantial increase of 221% for FSHIN8 due to the increase in the strength and elongation ratio values. This large increase could be attributed to the bimodal (micron and submicron) reinforced phase effect, where the nano-sized fumed silica particles and micron-sized fumed silica particles were integrated with hybrid IPN second phases.

3.2 | Thermal properties

Thermal properties are important for epoxy applications in terms of fire risk, and this is one of the major drawbacks of epoxies besides their fracture toughness.[16] Therefore, glass transition temperatures, thermal decomposition temperatures, and char yields of three different nanocomposites were examined. These values are given in Table 4.

It is well-known that there are various factors influencing the thermal properties of polymers such as the characteristic properties of chemical bonds, inorganic additives, and crosslinking density. For example, Si—O—Si bonds have a higher decomposition bonding energy than C—O, C—C, and C—NH bonds, respectively. Hence, it was expected that Si—O—Si bonds and inorganic particles would increase TGA values such as decomposition temperatures and char yields.

In the FSN samples, the maximum temperature at weight loss of 15% (T_{15}) reached 333°C for FSN10. The maximum char yield value of FSNs at 800°C was 16.6%. All plots of FSNs are given in Figure 7.

The second set of nanocomposite materials, namely SHINs, exhibited different trends as shown in Figure 7. While the T_{15} values of SHINs decreased continuously with an increase in their second phase content, their char yield values increased. The decrease at T_{15} varied from 291 to 230°C, and the increase in char yields varied from 5.7% to 8.4%. The decomposition temperature decrease in SHINs at T_{15} could be associated with the organic structure of the STU hybrid polymer network because of the low decomposition bonding energy of C—C and C═O. The increase in char yields could be explained by the Si—O—Si bonds in the hybrid structure.

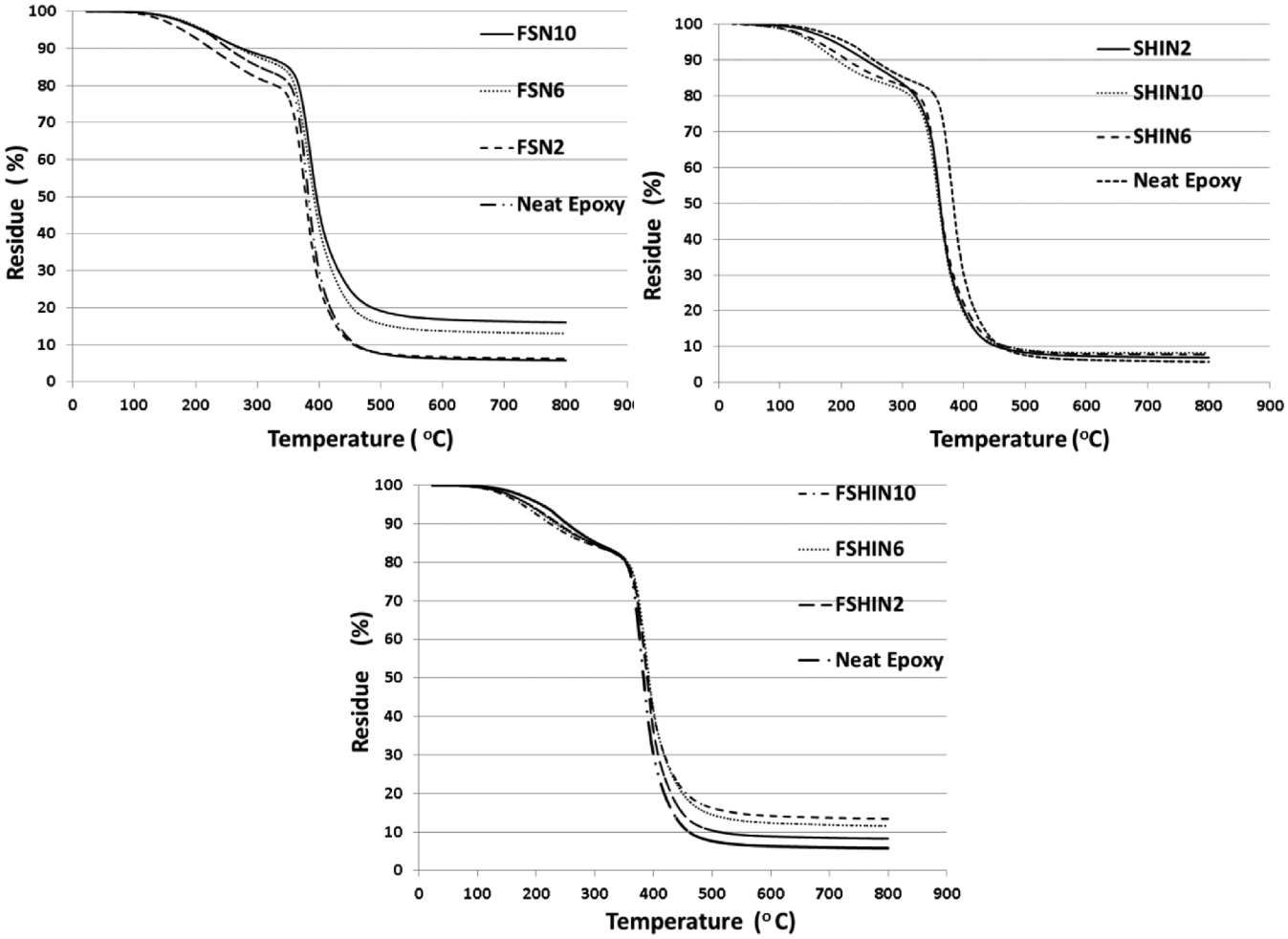

FIGURE 7 Thermogravimetric analysis curves of neat epoxy, FSNs, SHINs, and FSHINs.

The TGA values of FSHIN showed a similar trend with values between those of SHINs and FSNs due to their content of organic and inorganic structures. Therefore, it was aimed to eliminate the drawbacks of SHINs with the reinforcement of fumed silica particles incorporated into the STU hybrid polymer network. The T_{15} values of FSHINs were slightly lower compared to those of the neat epoxy. These values decreased from 291°C (neat epoxy value) to 281°C, 280°C, and 270°C for FSHIN2, FSHIN6, and FSHIN11, respectively. The char yield values improved significantly at rates of 8.2%, 11.5%, and 13.4%, respectively, compared with the neat epoxy.

Thermal glass transition refers to the mobilization of the transition from the glassy state to the liquid state in heating experiments. It was observed that the glass transition temperatures of three different nanocomposite materials improved substantially compared to those of the neat epoxy.

FSNs included only fumed silica particles as reinforcement additives as mentioned before. In the literature, most studies have revealed that neat fumed silica particles (without any compatibilizer or coupling agents) have weaker adhesion properties with epoxy than silica-siloxane particles obtained with the sol–gel process. Hence, the glass transition temperature values of neat fumed silica particle-reinforced epoxy systems present no considerable increase, or even a slight decrease.[17,18] Contrary to most studies in the literature, FSNs showed improved glass transition temperatures compared with the neat epoxy in this study, like the results in the studies conducted by Ou and Shiu.[19] FSN2, FSN4, and FSN6 showed T_g values of 64, 68, and 61°C, respectively. The maximum increase in T_g values was observed to be 62% compared with the neat epoxy. It can be deduced from these results that the fumed silica particles in the epoxy system exhibited high compatibility and adhesion properties between the matrix and the reinforcement. A large contact surface area of the fumed silica particles with the matrix is important to restrict segmental motion and increase T_g thanks to the good interfacial force between the matrix and the reinforcement.[17–19]

SHINs included inorganic and organic structures, which were provided by the STU polymer and Si—O—Si bonds. It was thought that SHINs produced an IPN with

Synthesis of STU polymer			
Components used for synthesis	Poly (hexamethylene carbonate) diol	3-Isocyanatopropyltrimethoxysilane (ICPTMS)	
Molar ratio	1 mole eq.	2 mole eq.	
Production of FSHINs			
Components used for synthesis	STU polymer	TEOS	Fumed silica
Molar ratio	1 mole eq.	4 mole eq.	
Weight ratio	2.65 wt. eq.	1 wt. eq.	1 wt. eq.
Production of SHINs			
Components used for synthesis	STU polymer	TEOS	None
Molar ratio	1 mole eq.	1 mole eq.	
Weight ratio	2.65 wt. eq.	1 wt. eq.	
Production of FSNs			
Components of FSNs	None	None	Fumed silica
Weight ratio			4.65 wt. eq.

TABLE 3 The molar and weight ratios of the reinforcement components.

Samples	T_g (°C)	Weight loss at T_{15} (°C)	Char yield (%)
EPOXY	42	291	5.7
FSN2	64	260	5.9
SHIN2	59	277	7.7
FSHIN2	62	281	8.2
FSN6	68	326	13.6
SHIN6	50	251	8.2
FSHIN6	64	280	11.5
FSN10	61	333	16.6
SHIN10	57	230	8.4
FSHIN10	61	270	13.4

TABLE 4 Thermal properties of the produced nanocomposites.

epoxy networks in the main structure. Hence, it was thought that Si—O—Si bonds also crosslinked with STU polymers. In the examinations of the effects of this structure on Tg, SHINs exhibited improved values of 59, 50, and 57°C for SHIN2, SHIN4, and SHIN6, respectively. SHINs had a maximum increase of 40% in T_g values compared with the neat epoxy. The characteristic T_g of poly hexamethylene carbonate is subzero. However, the crosslinking of the hexamethylene carbonate with the Si—O—Si bonds in the epoxy network (IPN system) increased the T_g of the neat epoxy. It was thought that this increase could have been associated with the higher degree of crosslinking in the structure due to the formation of IPNs. On the contrary, the glass transition peaks of SHINs were much broader than those of the neat epoxy as shown in Figure 8. Moreover, these peaks exhibited single glass transitions along the lines. The results showed that SHINs had a homogeneous structure despite the fact that the epoxy system included another organic–inorganic structure. Otherwise, more glass transition peaks could be observed in case of phase separation in IPN systems.[5,20]

FSHINs included both fumed silica particles and fumed silica-reinforced STU hybrid IPN polymer parts in the epoxy system. In the examinations of the T_g values, high T_g values were obtained as 62, 64, and 61°C compared with the neat epoxy. Moreover, these values were higher than the values of SHINs. Hence, the fumed silica particles contributed positively to the T_g values of SHINs. This increase in T_g values could be explained by the more prominent restriction of the motion of molecular chains.[19,20] Moreover, Figure 8 shows the difference of the peak curves in DSC between FSNs and FSHINs. The peaks of FSHINs were seen to be sharper than those of

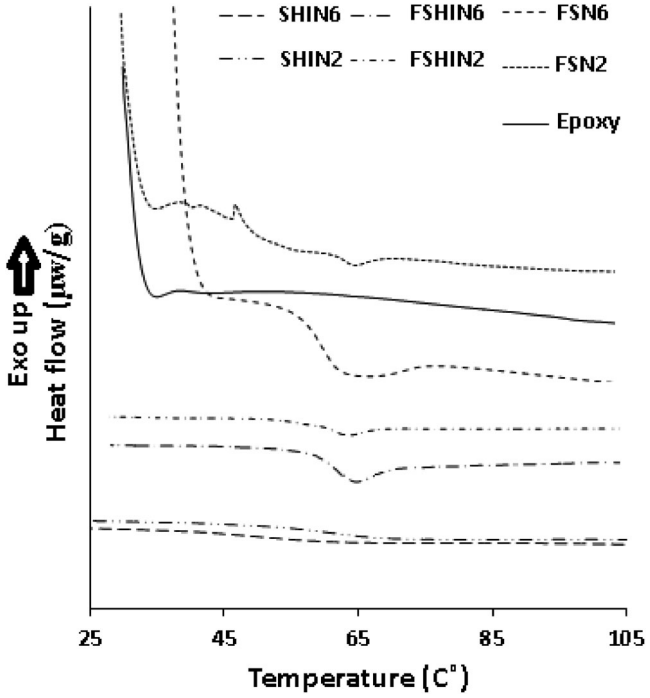

FIGURE 8 Differential scanning calorimetry curves of neat epoxy, FSN, SHIN, and FSHIN nanocomposites at ratios of 2% and 6%.

FSNs. It could be deduced from these results that the reinforcements in FSHINs were more compatible with the matrix due to the sharper peaks, but the soft segments could have reduced the T_g values of FSHINs slightly.

3.3 | Morphological analysis

The morphological analysis of the fracture surfaces for neat epoxy and three different nanocomposites (FSN, SHIN, and FSHIN) was performed by SEM. The fumed silica material showed favorable homogeneous dispersion, and the particle sizes for all samples are shown in Figure 9. Moreover, the fumed silica particles for FSNs showed little agglomeration with an increase in their content. While the particle size generally increased from 5–30 to 70 nm for all FSNs, some local agglomerations were observed, such as particle sizes ranging from 150 to 300 nm for FSN8 and FSN10. This situation could have reduced the tensile strength of FSNs for larger content values than 6% due to the decrease in contact surface area with the matrix.

As mentioned, an increase in the toughness of the epoxy system was provided with the STU hybrid network part and the integration of the fumed silica particles. Figure 9 also shows the whitening areas, which are the indicators of tough fractures for SHIN10. Moreover, the phase separation of the organic and inorganic parts for SHIN10 is given in Figure 9. Additionally, the residual char yields of SHINs in the TGA curves in Figure 7 are higher than the neat epoxy. This situation confirms the availability of inorganic parts in the IPN system. Regarding FSHINs, fracture surface and fumed silica-integrated organic–inorganic parts were given for FSHIN10 in Figure 9. There seemed to be different particle sizes at the nano scale. These fumed silica-integrated organic–inorganic parts showed an almost homogeneous distribution. This situation could be associated with the fumed silica nanoparticles surrounding the Si-O-Si network as shown in the schema in Figure 9.

Moreover, large dimples at the microscale were present. These dimple fractures could be an indicator of the STU hybrid polymer network in the epoxy network (IPN phases). These phases were important for increasing the toughness. The fumed silica particles with or without siloxane networks in this system formed as reinforcements and toughened the particles on a nano scale. It was observed that FSHINs had micron- and submicron-scale reinforcement and toughening phases, and the results confirmed this situation. It is believed that these microscale phases and submicron particles caused the formation of a crack-pinning effect. A crack-pinning mechanism is described as a process in which as a crack propagates through the matrix, the crack front bows out between the second IPN phases and nanoparticles and remains pinned at the positions where it has encountered the particles. In other words, toughening may occur through the interaction of moving crack fronts with both dispersed second IPN phases and nanoparticles. Nanoparticles and phases can act as barriers that pin a crack, and so, cause crack fronts to bow out between particles and IPN phases. During crack initiation, a new fracture surface is formed, and the length of the crack front increases.[21–23] On the contrary, it was thought that the fumed silica particles increased the rigidity and strength of the STU hybrid network. Hence, it was thought that IPN phases with high strength values were obtained, and the tensile strength of the neat epoxy was improved significantly 10 µ.

4 | CONCLUSION

In this study, it was aimed to enhance the mechanical and thermal properties of an epoxy system. In this regard, three different nanocomposite materials were obtained, including a fumed silica nanoparticle-reinforced epoxy nanocomposite (FSN), an epoxy/STU hybrid IPN nanocomposite (SHIN), and a fumed silica-reinforced epoxy/

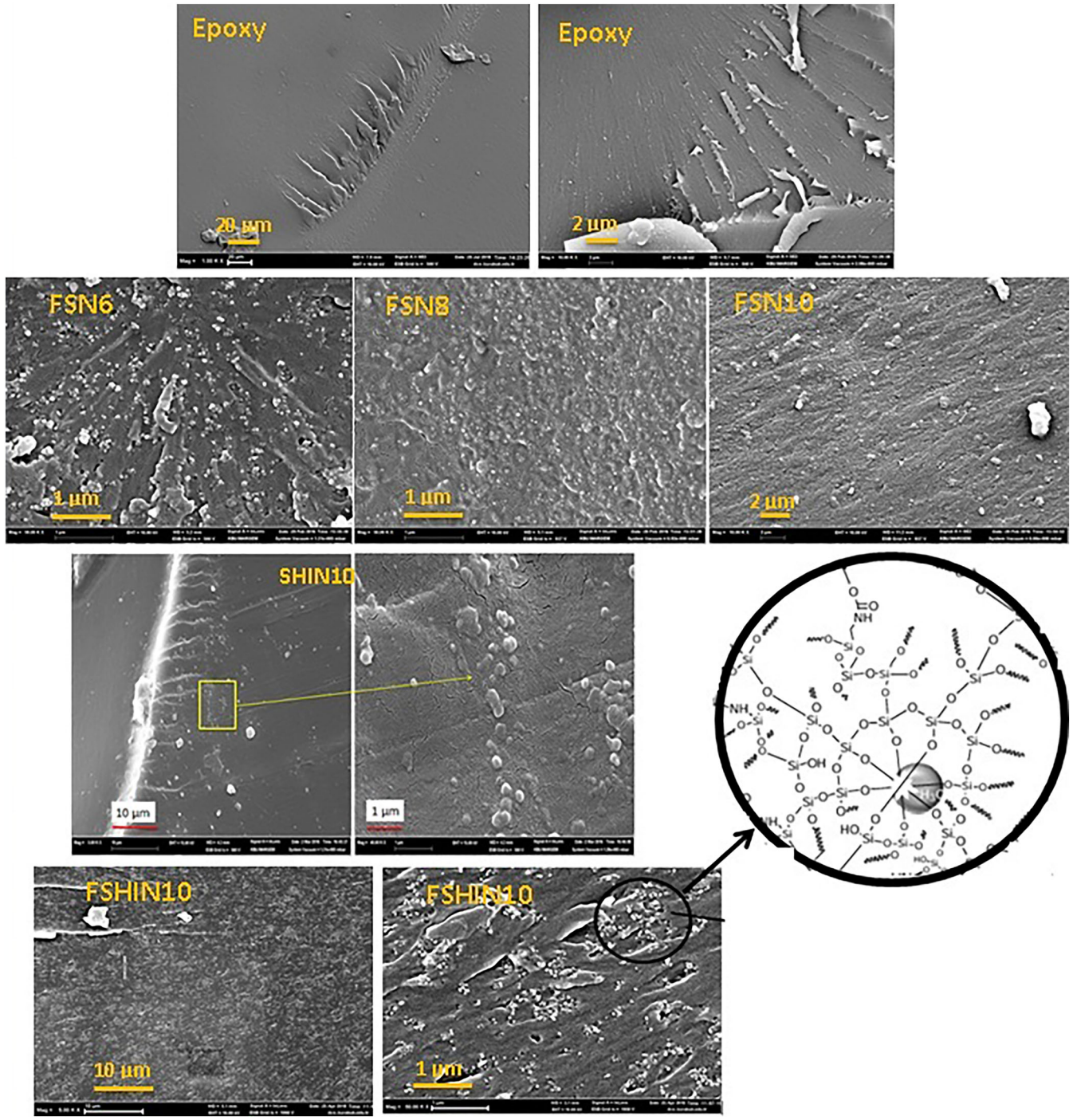

FIGURE 9 Scanning electron microscopy micrographs of fracture surfaces of neat epoxy and some FSN, SHIN, and FSHIN samples.

STU hybrid IPN nanocomposite (FSHIN), which exhibited more improved properties than the neat epoxy. Among these materials, the most prominent ones were FSHINs. In terms of mechanical properties, Young's modulus, ultimate tensile strength, and Izod impact resistance increased at rates of 53%, 50%, and 223%, respectively. As seen here, a large increase was observed in Izod impact resistance. This prominent increase could be associated with the crack-pinning effect between both IPN phases in micron and submicron sizes and the fumed silica particles in nano sizes. On the contrary, FSHINs exhibited improved properties in terms of char yields and T_g values. In addition to char yields and T_g values, the thermal decomposition temperature (T_d) values of FSHINs were considerably high and very close to the values of the neat epoxy. While the content of the fumed silica particles was effective in the increase in the T_d values, the organic part in the STU hybrid polymer network structure was effective in the decrease in the T_d values. Thus, FSNs exhibited high T_d values compared

with FSHINs due to their higher content of fumed silica (1/4.65 wt. for FSHIN/FSN) and the absence of an organic part in the STU hybrid polymer network structure. Furthermore, FSNs exhibited the highest char yield and Young's modulus values because of the same reasons. In the examinations of the T_g values, the values of all nanocomposites improved significantly compared to those of the neat epoxy. These increases were in the range between 40% and 62%. In summary, the fumed silica-reinforced IPN phases and the fumed silica nanoparticles in the epoxy system seemed to play a significant role in increasing the ultimate tensile strength and Izod impact resistance values. Besides these, the inorganic part obtained with the sol–gel process and the fumed silica nanoparticles also improved the thermal properties of the samples.

DATA AVAILABILITY STATEMENT

The data that support the findings of this study are available from the corresponding author upon reasonable request.

ORCID

Emre Akın https://orcid.org/0000-0003-2067-1488

REFERENCES

1. Hosseini SR, Nikje MMA. Synthesis and characterization of novelepoxy-urethanecoating and its graphene nanocomposites. *Polym Compos*. 2023;44:2794-2803.
2. Romo-Uribe A, Arcos-Casarrubias JA, Mayer AR, Guardian-Tapia R. PDMS nanodomains in DGEBA epoxy Induce high flexibility and toughness. *Polym-Plast Technol Eng*. 2017;56(1):96-107. doi:10.1080/03602559.2016.1211691
3. He W, Zhang Z, Wang R, et al. Effect of core–shell structured SiO_2@MoS_2 on the tribological properties of epoxy resin/carboxyl terminated butadiene acrylonitrile composites. *Polym Compos*. 2023;44:1252-1263.
4. Molaei A, Jannesari A. The synergistic impacts of hybrid nanofillers of graphene nanoplatelets/carbon nanotubes on curing behavior of an epoxy-vinyl ester interpenetrating polymer network nanocomposite coating. *Polym Compos*. 2023;44:7701-7726.
5. Özdemir H, Özbek Ö, Bozkurt ÖY, Erklig A. Buckling characteristics of nano-silica doped carbon fiber reinforced composites having cutouts. *Polym Compos*. 2024;45(8):7636-7646. doi:10.1002/pc.28293
6. Boztoprak Y, Çetin G, Şardan MZ, Kiliç SE, Kalender M. The effect of carbon nanotube addition on the mechanical properties of fiber reinforced composite materials. *J Math Eng Nat Sci*. 2019;3(10):41-51.
7. Kartal İ, Boztoprak Y. Investigation of mechanical properties of vinyl ester composites reinforced with boron nitride particles. *El-Cezerî J Sci Eng*. 2019;6(1):43-50.
8. Zidan TA. Synthesis and characterization of modified properties of poly(methyl methacrylate)/organoclay nanocomposites. *Polym Compos*. 2020;41:564-572.
9. Kesavulu A, Mohanty A. Investigation of physical, flexural, and dynamic mechanical properties of alumina and graphene nanoplatelets filled epoxy nanocomposites. *Polym Compos*. 2022;43:2711-2723.
10. Hao Q, Zhang X, Liu S, et al. Preparation of GO-SiO_2 three-dimensional point-plane nanomaterials and enhancement of epoxy resin mechanical property. *Polym Compos*. 2024;45:1266-1277.
11. Tilbrook MT, Moon RJ, Hoffman M. On the mechanical properties of alumina–epoxy composites with an interpenetrating network structure. *Mater Sci Eng A*. 2005;393:170-178.
12. Acebo C, Fernández-Francos X, Santos J-I, Messori M, Ramis X, Serra A. Hybrid epoxy networks from ethoxysilyl-modified hyperbranched poly(ethyleneimine) and inorganic reactive precursors. *Eur Polym J*. 2015;70:18-27.
13. Yilgor E, Eynur T, Kosak C, et al. Fumed silica filled poly(dimethylsiloxane-urea) segmented copolymers: preparation and properties. *Polymer*. 2011;52:4189-4198.
14. Marouf BT, Mai Y-W, Pearson RB. Toughening of epoxy nanocomposites: Nano and hybrid effects. *Polym Rev*. 2016;56(1):70-112.
15. Matejka L, Dusek K, Plestil J, Kriz J, Lednicky F. Formation and structure of the epoxy-silica hybrids. *Polymer*. 1998;40:171-181.
16. Chrusciel JJ, Lesniak E. Modification of epoxy resins with functional silanes, polysiloxanes, silsesquioxanes, silica and silicates. *Prog Polym Sci*. 2015;41:67-121.
17. Tarrio-Saavedra J, Lopez-Beceiro J, Naya S, Gracia C, Artiaga R. Controversial effects of fumed silica on the curing and thermomechanical properties of epoxy composites. *eXPRESS Polym Lett*. 2010;4(6):382-395.
18. Sipaut CS, Ahmad N, Adnan R, et al. Properties and morphology of bulk epoxy composites filled with modified fumed silica-epoxy nanocomposites. *J Appl Sci*. 2007;7(1):27-34.
19. Ou C-F, Shiu M-C. Epoxy composites reinforced by different size silica nanoparticles. *J Appl Polym Sci*. 2010;115:2648-2653.
20. Qingming J, Maosheng Z, Renjie S, Hongxiang C. The glass transition temperature and microstructure of polyurethane/epoxy resin interpenetrating polymer networks nanocomposites. *Chin Sci Bull*. 2006;51(3):293-298.
21. Sprenger S. Epoxy resins modified with elastomers and surface-modified silica nanoparticles. *Polymer*. 2013;54:4790-4797.
22. Kartal I. Toughening of epoxy resin via silane terminated urethane including pre-hydrolyzed tetraethoxysilane. *Asian J Chem*. 2014;26(18):6018-6022.
23. Demirer H, Kartal İ, Çakir M. Improvement of the surface properties of polystyrene sheets via UV curable organic-inorganic hybrid coatings. *Acta Phys Pol A*. 2017;131(3):555-558.

How to cite this article: Akın E, Çakır M, Kartal İ. Mechanical and thermal properties of fumed silica-incorporated silane-terminated urethane/epoxy-interpenetrating polymer network nanocomposites. *Polym Eng Sci*. 2024;1-15. doi:10.1002/pen.26817